Computers, Materials & Continua CMC, vol.64, no.2, pp.1139-1151, 2020

A High Gain, Noise Cancelling 2515-4900 MHz CMOS LNA for China Mobile 5G Communication Application

Xiaorong Zhao[1], Weili Cheng[2], Hongjin Zhu[1], Chunpeng Ge[3], Gengyuan Zhou[1, *] and Zhongjun Fu[1]

Abstract: With the development of the times, people's requirements for communication technology are becoming higher and higher. 4G communication technology has been unable to meet development needs, and 5G communication technology has emerged as the times require. This article proposes the design of a low-noise amplifier (LNA) that will be used in the 5G band of China Mobile Communications. A low noise amplifier for mobile 5G communication is designed based on Taiwan Semiconductor Manufacturing Company (TSMC) 0.13 μm Radio Frequency (RF) Complementary Metal Oxide Semiconductor (CMOS) process. The LNA employs self-cascode devices in current-reuse configuration to enable lower supply voltage operation without compromising the gain. This design uses an active feedback amplifier to achieve input impedance matching, avoiding the introduction of resistive negative feedback to reduce gain. A common source (CS) amplifier is used as the input of the low noise amplifier. In order to achieve the low power consumption of LNA, current reuse technology is used to reduce power consumption. Noise cancellation techniques are used to eliminate noise. The simulation results in a maximum power gain of 22.783, the reverse isolation (S_{12}) less than -48.092 dB, noise figure (NF) less than 1.878 dB, minimum noise figure (NFmin)=1.203 dB, input return loss (S_{11}) and output return loss (S_{22}) are both less than -14.933 dB in the frequency range of 2515-4900 MHz. The proposed Ultra-wideband (UWB) LNA consumed 1.424 mW without buffer from a 1.2 V power supply.

Keywords: Common source, low noise amplifier, current reuse, noise cancelling.

1 Introduction

As the requirements for spectrum utilization and throughput of mobile network communication continue to increase, 5G mobile communication technology with high-speed data transmission rate has become a research hotspot [Park, Choi, Kim et al. (2015); Ren, Zhu, Sharma et al. (2020)]. 5G wireless communication covers multiple frequency bands, such as low frequency band less than 1 GHz, medium frequency band

[1] College of Computer Engineering, Jiangsu University of Technology, Changzhou, 213001, China.

[2] Jiangsu Agri-Animal Husbandry Vocational College, Taizhou, 225300, China.

[3] University of Wollongong, Wollongong, NSW 2522, Australia.

[*] Corresponding Author: Gengyuan Zhou. Email: zgy432698@sina.com.

Received: 18 February 2020; Accepted: 18 April 2020.

of 1-6 GHz and high frequency band above 24 GHz [Kishore, Rajan, Sanjay et al. (2019); Park, Choi, Kim et al. (2015)]. The LNA is a module at the forefront of the RF receiver, Its main function is to suppress noise and amplify the useful signal received from the antenna [Ge, Liu, Xia et al. (2019); Ge, Susilo, Fang et al. (2018); Mao, Zhang, Qi et al. (2019)]. The LNA should meet input impedance matching in a specific high frequency range, introduce low noise as much as possible, have a flat gain, and must have sufficient linearity to accommodate possible signal energy variations [Baumgratz, Saavedra, Steyaert et al. (2019); Zhao, Liu, Guo et al. (2018)]. Therefore, the overall performance of the receiver is directly related to the performance of the LNA's noise, matching, and linearity [Zhao, Zhu, Shi et al. (2019); Li, Yan, Chen et al. (2019)]. With the development of technology, people have higher and higher requirements for communication [Lu and Feng (2018)]. Therefore, designing a broadband low-noise amplifier with high gain and low noise is the key to realize 5G wireless communication system [Fan and Zhu (2018a); Zhu, Fan, Shu et al. (2019)].

In designing a low noise amplifier, the researchers provided many CMOS technologies and topologies such as current reused amplifiers [Lin, Hsu, Jin et al. (2007); Fan and Zhu (2018b)]. The use of current multiplexing technology is used for power consumption reduction, but the noise performance is not improved, and the noise will become larger due to the use of current utilization technology [Qu, Li, Xu et al. (2019); Fan and Zhu (2018c)]. Chirala et al. [Chirala, Guan and Nguyen (2006)] have reported the distributed amplifie, the structure can achieve good input wideband matching, but it needs to consume a lot of power [Lee, Park, Chang et al. (2012)]. Chen et al. [Chen, Lu, Chen et al. (2007)] have introduced the cascade amplifiers, the structure can be reasonably connected in series according to the circuit characteristics, thereby achieving the design goal. Therefore, in order to reduce the NF of the low noise amplifier, Khurram et al. [Khurram and Hasan (2011)] have proposed the noise cancellation technology. Self-cascode (SC) Metal-Oxide-Semiconductor Field-Effect Transistor (MOSFET) can give better g_m and r_{out} characteristics, thus enhancing the circuit performance [Baek, Gim, Kim et al. (2013)]. Xu et al. [Xu, Liu and Xu (2016)] have introduced operational transconductance amplifiers (OTAs) which can achieve higher gains, and in LNAs as a cascode block for bandwidth enhancement and gain [Pandey, Gawande and Kondekar (2018); Kishore, Venkataramani, Sanjay et al. (2019)].

2 Circuit design and analysis

2.1 Circuit design and analysis

The input stage design of the UWB LNA is critical for forward gain, input matching, and low noise performance. Well-known CS and common gate (CG) topologies are widely used by designers for UWB LNA input stages. Khurram et al. [Khurram and Hasan (2011); Zhang, Fan and Sinencio (2009); Ponton, Palestri, Esseni et al. (2009)]. When the CG structure is used in the input stage design, impedance matching can be achieved over a wide frequency band by reasonable circuit operating current and transistor size selection [Bastos, Oliveira, Goes et al. (2016); Wan, Chen and Zhang (2019)]. Noise cancellation techniques can be used to optimize circuit noise in specific circuit design, but the use of noise cancellation techniques requires additional circuitry, resulting in increased circuit power consumption, and in order to achieve cross-conductance g_m=1/50 Ω power matching, noise

is inevitable. In addition, in order to achieve perfect matching of transconductance gm = 1 / 50 Ω, which ultimately leads to loss of flexibility in circuit design. Li et al. [Li, Wang, Zhang et al. (2014)] have reported that common-gate structure is combined with g_m-boosting and current-reuse techniques that leads to increase the gain. However, the NF of this design is still high [Daryabari, Zahedi, Rezaei et al. (2019)]. When the input terminal adopts the CS structure, the NF can be made small, but in order to achieve low noise, it must pay a great power cost. The noise reduction techniques are used in CS structure but the design suffers from narrow bandwidth and low IIP3. To increase the linearity of LNA, feed-back structures can be used. Huang et al. [Huang, Yang, Chen et al. (2018)] have used active feedback to increase the linearity of LNA.

The resistor negative feedback technique can be used to extend the operating band-width of the circuit. The input and output matching in the wideband range can be achieved by reasonably selecting the feedback resistor RF and determining the equivalent transconductance of the circuit. However, due to the introduction of a negative feedback resistor, the gain of the circuit is reduced, and for input matching, the circuit noise cannot be improved by transconductance [Ma and Hu (2019)]. The stability of the structure circuit is greatly affected, and the circuit cannot achieve effective matching. The resistor LNA in the figure achieves input matching by connecting a resistor in parallel with the gate drain of the Metal-Oxide-Semiconductor (MOS) transistor. The resistive negative feedback amplifier schematic shown in Fig. 1, the input impedance is:

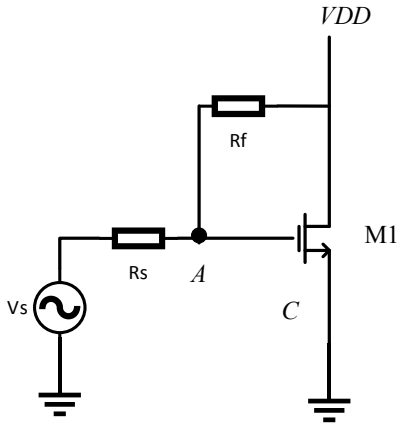

Figure 1: Resistive negative feedback amplifier schematic

$$Z_{\text{in}} = 1/g_m \tag{1}$$

In order to achieve input matching, g_m needs to be set to 20 mS. When the input impedance matches, the gain of the resistor feedback LNA is:

$$A_v = \frac{v_{out}}{v_{in}} = 1 - g_m R_f \approx \frac{R_f}{R_s} \tag{2}$$

The noise factor of the resistance feedback LNA can be expressed by the Eq. (3):

$$F = 1 + \frac{4R_f}{R_s(1 - R_f / R_s)^2} + \frac{\gamma g_m (R_f + R_s)^2}{R_s(1 - R_f / R_s)^2} \approx 1 + \frac{4}{A_v} + \gamma \tag{3}$$

Here γ is the thermal noise coefficients of M1 and M2. It can be seen from the Eq. (3) that this noise performance is very general.

The complete circuit structure diagram of the UWB LNA proposed in this paper is shown in the Fig. 2. The circuit uses CS structure as the input and input feedback through M3, which can avoid the introduction of resistance negative feedback and reduce the gain, and can achieve the purpose of expanding the bandwidth. M1 and M2 use a common source and common shed structure. The inductor L1 prevents high-frequency AC signals from flowing through, but ensures that DC power passes. M2 and M4 use current utilization technology, which can reduce the power consumption of the circuit.

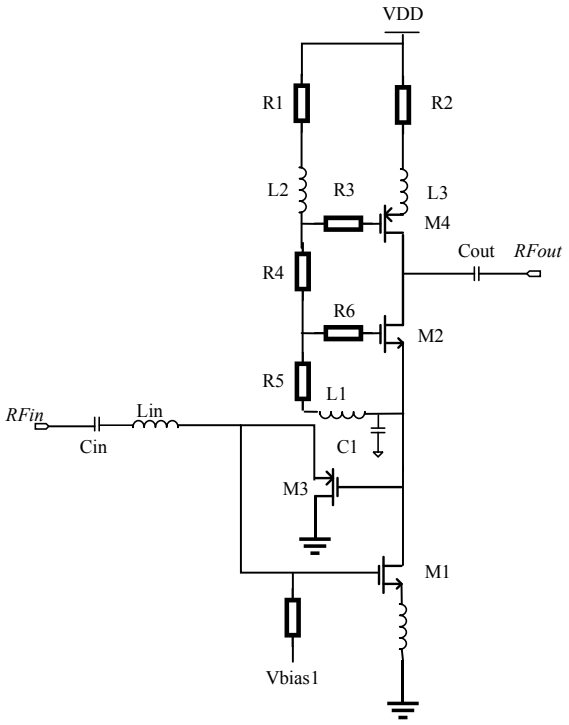

Figure 2: Proposed low power, noise canceling schematic

All MOS transistors use forward substrate bias technology to achieve low voltage and reduce circuit power consumption while maintaining MOS transistors with device characteristics. In this paper, active feedback is used as the input end of the LNA. The active feedback LNA can break the constraint be-tween the matching and the noise received by the resistance feedback LNA. The gain is provided by the CS level and can be expressed by the Eq. (4):

$$A_v = -g_m R_f \tag{4}$$

The input impedance can be expressed by the Eq. (5):

$$Z_{in} = \frac{g_{m2}^{-1}}{1 - A_v} \tag{5}$$

Here g_{m1} and g_{m2} are transconductances of M1 and M2, respectively.

When the input matches, the noise factor of the active feedback LNA is:

$$F = 1 + \left(\frac{2 - A_v}{1 - A_v}\right)^2 \bullet \frac{1}{g_{m1} R_s} \bullet \left(\gamma + \frac{1}{A_v}\right) + \frac{\gamma}{1 - A_v} \tag{6}$$

It can be seen from the Eq. (6) that the transconductance g_{m1} of the CS amplifier M1 of the active feedback LNA is not limited by the input matching compared to the resistance feedback LNA. Therefore, noise performance can be improved by increasing g_{m1}. The active feedback LNA can independently design gain, match, and noise, adding one design freedom to the resistive feedback LNA.

2.2 Noise analysis

In the receiver circuit, most of the unit circuits, such as filters and low-noise amplifiers, can be regarded as a two-port network. The RF signals pass through each net-work step by step, and the entire receiver can be equivalent to cascade of multiple networks [Wang, Shao, Gao et al. (2019)]. An effective way to effectively estimate the overall noise figure (F_{TOTAL}) of a computer-cascaded two-port network is to use the Friss formula:

$$F_{TOTAL} = F_1 + \frac{F_2 - 1}{G_1} + \frac{F_3 - 1}{G_1 G_2} + \cdots \tag{7}$$

where F_1, F_2 and F_3 represent the first, second and third level noise, while G_1 and G_2 represent the gain of the first and second stage amplifiers, respectively. It can be known from the Friss formula that the NF of the pre-stage circuit has the greatest influence on the overall NF. If the gain of the first-stage circuit is sufficiently large, the overall NF is only slightly larger than the NF of the first-stage circuit. If the overall NF of the second and subsequent circuits is NF_{OTHER}, the overall NF of the system is:

$$F_{TOTAL} = F_1 + F_{OTHER} \tag{8}$$

When the entire receiver circuit is simplified, the circuit of the LNA stage is replaced by an integral module as shown Fig. 3. The overall noise figure F_{TOTAL} of the receiver is:

$$F_{TOTAL} = F_{LNA} + \frac{F_{OTHER} - 1}{G_{LNA}} \tag{9}$$

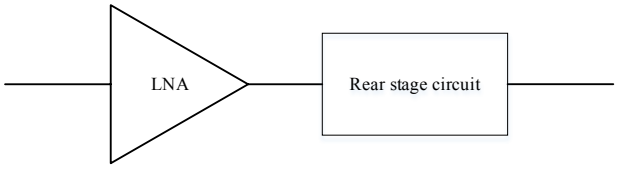

Figure 3: Receiver simplified structure diagram

Assume that the parameters of the receiver are as follows: F_{LNA}=3 dB≈1.995， G_{LNA}=20 dB=100， F_{OTHER}=9 dB≈7.943. According to formula 9, F_{TOTAL}=2.064 dB. In the calculation process, the contribution of the NF of each level of circuit to the overall NF is shown in the Tab. 1:

Table 1: The contribution of the NF of each level of circuit to the overall NF

	LNA	Rear stage circuit	Receiver overall
Noise	1.995	7.943	2.064
Contribution to F_{TOTAL}	1.995	0.069	2.064
Proportion of F_{TOTAL}	96.66%	3.34%	

It can be seen from the data in the table that although the NF of the latter circuit itself is larger than that of the LNA, its contribution to the NF of the overall receiver is small. When the gain of the LNA is increased, the proportion of the latter circuit is smaller. Therefore, in the receiver circuit, the LNA's own NF is decisive for the overall noise of the receiver.

The input circuit of the low noise amplifier and the noise analysis diagram are shown in the Fig. 4. Since the noise of the multi-stage low noise amplifier is mainly generated by the first-stage transistor M1, the noise of the low-noise amplifier can be almost eliminated if the noise generated by the transistor M1 is eliminated. Since the noise of the transistor M1 is mainly generated by the M1 channel current, assuming that the noise current generates a noise voltage of -Vn at the node B in the figure, the noise voltage -Vn generates a noise voltage of -aVn at the node A via the transistor M3. The noise -aVn, through transistor M1, again produces a noise voltage of abVn at node B. Since the noise voltage of abVn and the noise voltage of -Vn are opposite in polarity, the noise voltage passing through the transistor M2 is (ab-1)Vn, and it is understood that when ab=1, the noise voltage passing through M2 is 0, thereby achieving the purpose of eliminating the noise generated by the transistor M1.

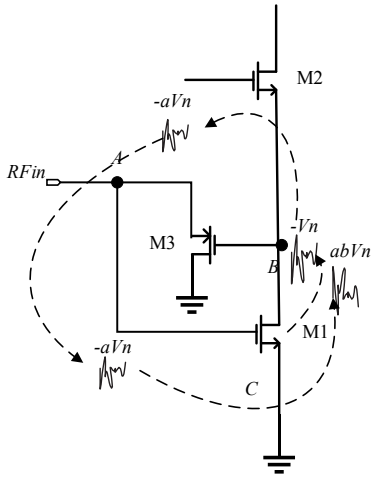

Figure 4: Low noise amplifier input circuit and noise analysis diagram

On the other hand, for the signal, the input circuit and signal analysis diagram of the low noise amplifier are shown in the Fig. 5. The input signal is RFin through transistor M1 to generate -b RFin signal at node B, and then a signal of size abRFin is generated at node A via transistor M3. Since the ab RFin and the input signal RFin have the same polarity, the signal will only increase and not cancel when it reaches the transistor M2. Therefore, the designed input circuit can achieve the effect of amplifying the input signal and

eliminating the noise generated by the input terminal transistor M1.

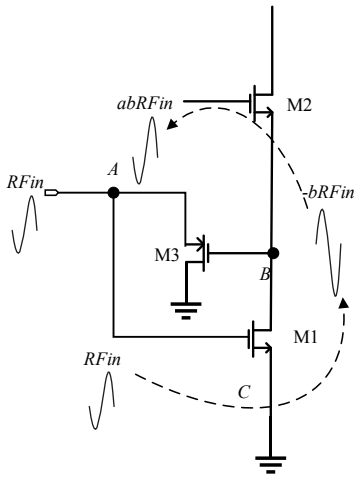

Figure 5: Low noise amplifier input circuit and signal analysis diagram

2.3 Current reused techniques

In order to achieve low power consumption of the circuit, this paper uses current multiplexing technology. The circuit diagram of the Self-Cascode LNA is shown in Fig. 2. M2 and M3 form a current reused configuration which enhances the effective trans-conductance. Due to the Self-Cascode structure, the designed LNA output resistance is large, so that the gain can be improved. In the Fig. 2, the current reused structure (M2) reduces power dissipation.

2.4 Stability

For the design of low noise amplifiers, in addition to factors such as gain, power consumption, noise, etc., the stability of the circuit design needs to be considered [Xu, Zhang, Fu et al. (2019)]. Oscillation may occur in extreme cases where current may vary in current or voltage, and may oscillate at unexpected high or low frequencies. The stability factor K is given by the Eq. (10) [Zhao, Zhu, Shi et al. (2019)]:

$$K = \frac{1 - |S_{11}|^2 - |S_{22}|^2 + |\Delta|^2}{2|S_{12}S_{21}|} \tag{10}$$

$$\Delta = S_{11}S_{22} - S_{12}S_{21} \tag{11}$$

As per Stern stability analysis, when the stability factor (K) is>1 and Δ<1 over the full frequency band, the LNA is unconditional stability [Zhao, Zhu, Shi et al. (2019)].

3 Analytical and circuit simulation results

The simulation results of the proposed LNA are shown in Figs. 6-9. which is simulated with Agilent Advanced Design System (ADS) tools. Fig. 6 shows the simulated S_{21} and S_{12} against frequency characteristics of the LNA. It can be seen from the Fig. 5 that the

maximum S_{21} can reach 22.783 dB and the minimum gain can reach 22.149 dB. The gain is very flat. The S_{12} is less than -45.528 dB, reverse isolation is very good. As shown in Fig. 7, the S_{11}<-11.441 dB and the output reflection coefficient $\mathbf{S_{22}}$<-7.646 dB. Fig. 8 shows the simulated NF against frequency characteristics of the proposed LNA. The lowest noise is only 1.203 dB, and the maximum noise is only 1.878 dB. Therefore, the noise cancellation technology used is very effective. It can be seen from Fig. 9 that the stability factor (K) is greater than 1 over the entire frequency band, so the designed low noise amplifier is stable. With a power supply of 1.2 V, the proposed circuit consumes 1.548 mW without buffer.

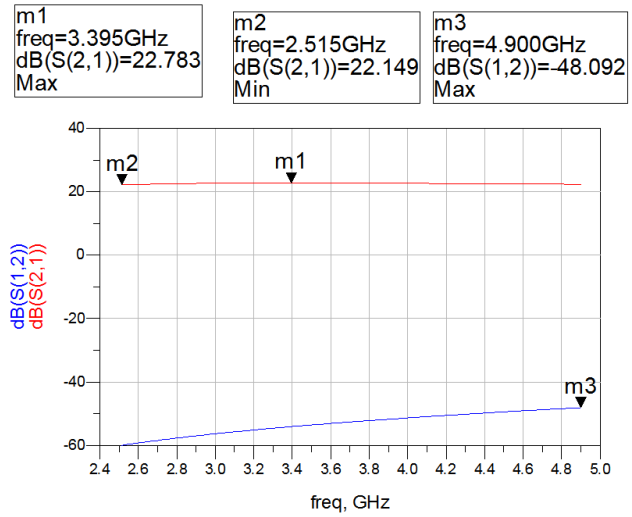

Figure 6: Simulated $\mathbf{S_{21}}$ and $\mathbf{S_{12}}$ against frequency characteristics

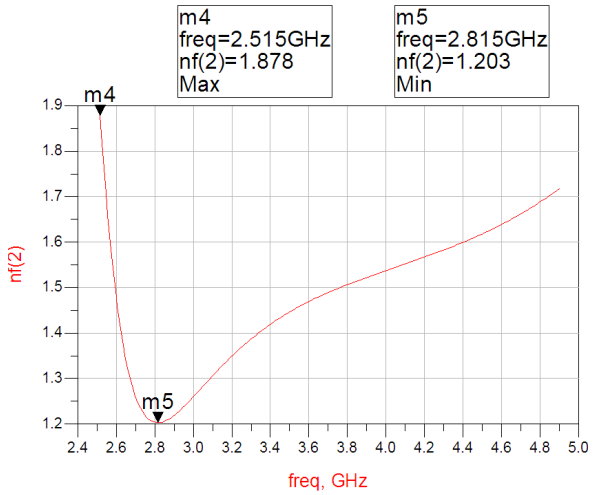

Figure 7: Simulated NF against frequency characteristics

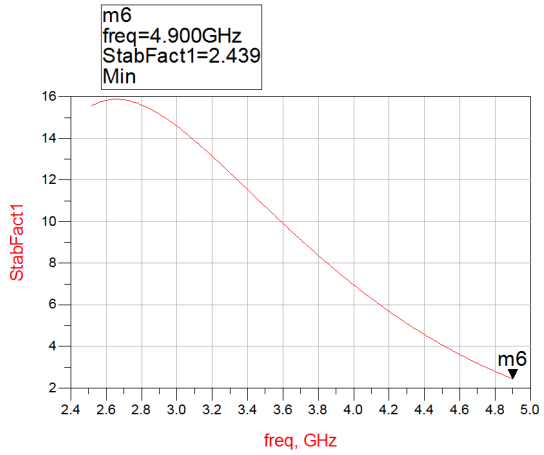

Figure 8: Simulated stability factor against frequency characteristics

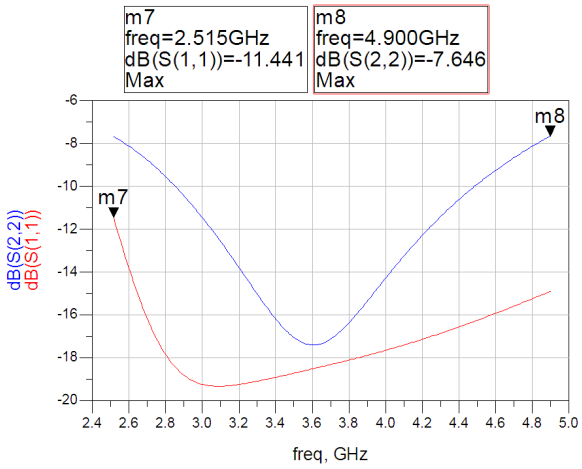

Figure 9: Simulated S_{11} and S_{22} against frequency characteristics

Table 2: Compare with simulation results of LNA from other recently published papers

	Tech. (μm)	BW (GHz)	S_{21} (dB)	NF (dB)	P_D (mW)	FOM (GHz/mW)
This work	0.13	2.515-4.9	22.297±1.487	1.541±0.338	1.424	69.9
[Kishore, Rajan, Sanjay et al. (2019)]	0.065	3.1-4.7	17.6#	2.2M	0.97	24.19
[Kishore, Venkataramani, Sanjay et al. (2019)]	0.18	0.18-2.0	20.8#	2.65M	4.9	4.84
[Huang, Yang, Chen et al. (2018)]	0.18	0.3-3.5	14.6 #	2.9 M	14.8	1.66

[Ma and Hu (2019)]	0.13	0.7-4.6	10.8#	3.5 M	6.16	2.74
[Kumar, Sahoo and Dutta (2018)]	0.18	2-5	13#	6M	1.8	4.33
[Regulagadda, Sahoo, Dutta et al. (2019)]	0.065	0.04-2.9	20#	2 M	29	8.16

* Average value

Maximum value

M Minimum value

Tab. 2 lists the low noise amplifier performance specifications designed in this paper and designed by researchers in recent years. By comparison, it can be found that the proposed low noise amplifier can achieve high gain and low noise. The proposed LNA exhibits higher FOM compared to other LNAs. The FOM is defined as Eq. (12) [Lin, Hsu, Jin et al. (2007)]:

$$FOM = \frac{|S_{21}| * BW}{(|NF| - 1) * P_D} \tag{12}$$

where $|S_{21}|$ represents the average power gain in magnitude; BW represents the bandwidth in GHz, |NF| represents the average NF in magnitude; and PD represents the power dissipation in milliwatts (mW). The FOM of the proposed UWB LNA achieves considerably high compared to most of the recently published popular designs. The proposed LNA can achieve a high and flat gain, low NF.

4 Conclusion

The paper reports a low power, high gain, low NF 2.515-4.9 GHz CMOS CS LNA, which adopts active feedback for input impedance matching and noise cancellation to eliminate noise, current reused technique to reduce power consumption, self-cascode technique to improve gain, designed using TSMC 0.13 μm RF CMOS technology. Simulation results show that the proposed low noise amplifier can achieve a high and flat gain of 22.297±1.487 dB, a low and flat NF of 2.169±0.448 dB, S_{12} less than -48.929 dB, S_{11} less than -11.441 dB and output $\mathbf{S_{22}}$ less than -7.646 dB, the stability factor more than 2.439 over bandwidth of 2.515-4.9 GHz, the LNA consumes 1.424 mW without buffer from a 1.2 V power supply. This structure is combined with post-distortion technique to increase the linearity of the circuit. The proposed structure has wide input matching and high IIP3 which suffers from high gain and low NF. The low noise amplifier designed in this paper can provide a good choice for China Mobile's 5G communication, and provide some ideas for low noise amplifier design researchers.

Funding Statement: This work was financially supported by the National Natural Science Foundation (No. 61806088), Jiangsu Province Industry-University-Research Cooperation Project (No. BY2018191), Natural Science Fund of Changzhou (CE20175026) and Qing Lan Project of Jiangsu Province.

Conflicts of Interest: The authors declare that they have no conflicts of interest to report regarding the present study.

References

Baek, K. J.; Gim, J. M.; Kim, H. S.; Na, K. Y.; Kim, N. S. et al. (2013): Analogue circuit design methodology using self-cascode structures. *Electronics Letters*, vol. 49, no. 9, pp. 591-592.

Bastos, I.; Oliveira, L. B.; Goes, J.; Oliveira, J. P.; Silva, M. (2016): Noise canceling LNA with gain enhancement by using double feedback. *Integration, the VLSI Journal*, vol. 52, pp. 309-315.

Baumgratz, F. D.; Saavedra, C.; Steyaert, M.; Tavernier, F.; Bampi, S. (2019): A wideband low-noise variable-gain amplifier with a 3.4 dB NF and up to 45 dB gain tuning range in 130-nm CMOS. *IEEE Transactions on Circuits and Systems II: Express Briefs*, vol. 66, no. 7, pp. 1104-1108.

Chen, K. H.; Lu, J. H.; Chen, B. J.; Liu, S. L. (2007): An ultra-wide-band 0.4-10 GHz LNA in 0.18 μm CMOS. *IEEE Circuits and Systems*, vol. 54, no. 3, pp. 217-221.

Chirala, M. K.; Guan, X.; Nguyen, C. (2006): Dc-20 GHz CMOS lima using novel multilayered transmission lines and inductors. *Electronics Letters*, vol, 42, no. 2, pp. 1273-1275.

Daryabari, F.; Zahedi, A.; Rezaei, A.; Hayati, M. (2019): Gain-controlled noise-reduction LNA design using source-bulk resistors and double common-source topology. *Integration*, vol. 68, pp. 50-61.

Fan, H. H.; Zhu, H. J. (2018a): Separation of vehicle detection area using Fourier descriptor under Internet of Things monitoring. *IEEE Access*, vol. 6, pp. 47600-47609.

Fan, H. H.; Zhu, H. J. (2018b). Preservation of image edge feature based on snowfall model smoothing filter. *EURASIP Journal on Image and Video Processing*, vol. 2018, no. 1, pp. 67.

Fan, H. H.; Zhu, H. J. (2018c): Improved image reconstruction based on ultrasonic transmitted wave computerized tomography on concrete. *EURASIP Journal on Image and Video Processing*, vol. 2018, no. 1, pp. 129.

Ge, C. P.; Liu, Z.; Xia, J.; Fang, L. M. (2019): Revocable identity-based broadcast proxy re-encryption for data sharing in clouds. *IEEE Transactions on Dependable and Secure Computing*. https://ieeexplore.ieee.xilesou.top/abstract/document/8642350.

Ge, C. P.; Susilo, W.; Fang, L. M.; Wang, J. D.; Shi, Y. Q. (2018): A CCA-secure key-policy attribute-based proxy re-encryption in the adaptive corruption model for dropbox data sharing system. *Designs, Codes and Cryptography*, vol. 86, no. 11, pp. 2587-2603.

Huang, D.; Yang, X. F.; Chen, H. F.; Khan, M. I.; Lin, F. J. (2018): A 0.3-3.5 GHz active-feedback low-noise amplifier with linearization design for wideband receivers. *AEU-International Journal of Electronics and Communications*, vol. 84, pp. 192-198.

Khurram, M.; Hasan, S. R. (2011): Novel analysis and optimization of g_m-boosted common-gate uwb LNA. *Microelectronics Journal*, vol. 42, no. 2, pp. 253-264.

Kishore, K. H.; Rajan, V. S.; Sanjay, R.; Venkataramani, B. (2019): Reconfigurable low voltage low power dual-band self-cascode current-reuse quasi-differential LNA for 5G. *Microelectronics Journal*, vol. 92, no. 3, pp. 1-9.

Kishore, K. H.; Venkataramani, B.; Sanjay, R.; Rajan, V. S. (2019): High-gain inductorless wideband balun-LNA using asymmetric ccc & bist using rms detectors. *AEU-International Journal of Electronics and Communications*, vol. 105, pp. 135-144.

Kumar, A. R. A.; Sahoo, B. D.; Dutta, A. (2018): A wideband 2-5 GHz noise canceling subthreshold low noise amplifier. *IEEE Transactions on Circuits and Systems II: Express Briefs*, vol. 65, no. 7, pp. 834-838.

Lee, J. Y.; Park, H. K.; Chang, H. J.; Yun, T. Y. (2012). Low-power UWB LNA with common-gate and current-reuse techniques. *IET Microwaves, Antennas and Propagation*, vol. 6, no. 7, pp. 793-799.

Li, G. S.; Yan, J. H.; Chen, L.; Wu, J. H.; Lin, Q. Y. et al. (2019): Energy consumption optimization with a delay threshold in Cloud-Fog cooperation computing. *IEEE Access*, vol. 7, no. 1, pp. 159688-159697.

Li, Z. Q.; Wang, Z. Q.; Zhang, M.; Chen, L.; Wu, C. J. et al. (2014): A 2.4 GHz ultra-low-power current-reuse CG-LNA with active g_m-boosting technique. *IEEE Microwave and Wireless Components Letters*, vol. 24, no. 5, pp. 348-350.

Lin, Y. J.; Hsu, S. S.; Jin, J. D.; Chan, C. Y. (2007): A 3.1-10.6 GHz ultra-wideband CMOS low noise amplifier with current-reused technique. *IEEE Microwave and Wireless Components Letters*, vol. 17, no. 3, pp. 232-234.

Lu, Y.; Feng, T. (2018): Research on trusted dnp3-bae protocol based on hash chain. *EURASIP Journal on Wireless Communications and Networking*, vol. 2018, no. 1, pp. 1-10.

Ma, T.; Hu, F. (2019): A wideband flat gain low noise amplifier using active inductor for input matching. *IEEE Transactions on Circuits and Systems II: Express Briefs*, vol. 66, no. 6, pp. 904-908.

Mao, Y. C.; Zhang, J. H.; Qi, H.; Wang, L. B. (2019): DNN-MVL: DNN-multi-view-learning-based recover block missing data in a dam safety monitoring system. *Sensors*, vol. 19, no. 13, pp. 2895.

Pandey, S.; Gawande, T.; Kondekar, P. N. (2018): A 3.1-10.6 GHz UWB LNA based on self cascode technique for improved bandwidth and high gain. *Wireless Personal Communications*, vol. 101, no. 4, pp. 1867-1882.

Park, H. S.; Choi, Y. S.; Kim, B. C.; Lee, J. Y. (2015): LTE mobility enhancements for evolution into 5G. *ETRI Journal*, vol. 37, no. 6, pp. 1065-1076.

Ponton, D.; Palestri, P.; Esseni, D.; Selmi, L.; Tiebout, M. et al. (2009): Design of ultra-wideband low-noise amplifiers in 45-nm CMOS technology: comparison between planar bulk and SOI FinFet devices. *IEEE Transactions on Circuits and Systems I: Regular Papers*, vol. 56, no. 5, pp. 920-932.

Qu, Z. G.; Li, Z. Y.; Xu, G.; Wu, S. Y.; Wang, X. J. (2019): Quantum image steganography protocol based on quantum image expansion and Grover search algorithm. *IEEE Access*, vol. 7, pp. 50849-50857.

Regulagadda, S. S.; Sahoo, B. D.; Dutta, A.; Varma, K. Y.; Rao, V. S. (2019): A packaged noise-canceling high-gain wideband low noise amplifier. *IEEE Transactions on Circuits and Systems II: Express Briefs*, vol. 66, no. 1, pp. 11-15.

Ren, Y. J.; Zhu, F. J.; Sharma, P. K., Wang, T., Wang, J. et al. (2020): Data query mechanism based on hash computing power of blockchain in Internet of Things. *Sensors*, vol. 20, no. 1, pp. 207.

Wan, W. N.; Chen, J.; Zhang, S. B. (2019): A cluster correlation power analysis against double blinding exponentiation. *Journal of Information Security and Applications*, vol. 48, no. 10, pp. 1-8.

Wang, C. X.; Shao, X.; Gao, Z.; Zhao, C. X.; Gao, J. (2019): Common network coding condition and traffic matching supported network coding aware routing for wireless multihop network. *International Journal of Distributed Sensor Networks*, vol. 15, no. 6, pp. 1-20.

Xu, D. G.; Liu, L.; Xu, S. L. (2016): High DC gain self-cascode structure of OTA design with bandwidth enhancement. *Electronics Letters*, vol. 52, no. 9, pp. 740-742.

Xu, J.; Zhang, Y. J.; Fu, K. Y.; Peng, S. (2019): Sgx-based secure indexing system. *IEEE Access*, vol. 7, pp. 77923-77931.

Zeng, S. K.; Mu, Y.; He, M. X.; Chen, Y. (2018): New approach for privacy-aware location-based service communications. *Wireless Personal Communications*, vol. 101, no. 2, pp. 1057-1073.

Zhang, H.; Fan, X. H.; Sinencio, E. S. (2009): A low-power, linearized, ultra-wideband LNA design technique. *IEEE Journal of Solid-State Circuit*, vol. 44, no. 2, pp. 320-330.

Zhao, W.; Liu, J. J.; Guo, H. Z.; Hara, T. (2018): ETC-IoT: Edge-node-assisted transmitting for the cloud-centric Internet of Things. *IEEE Network*, vol. 32, no. 3, pp. 101-107.

Zhao, X. R.; Zhu, H. J.; Shi, P. Z.; Ge, C. P.; Qian, X. F. et al. (2019): A high gain, noise cancelling 3.1-10.6 GHz CMOS LNA for uwb application. *Computers, Materials & Continua*, vol. 60, no. 1, pp. 133-145.

Zhu, H. J.; Fan, H. H.; Shu, Z. Q.; Yu, Q.; Zhao, X. R. et al. (2019). Edge detection with chroma components of video frame based on local autocorrelation. *IEEE Access*, vol. 7, pp. 48543-48550.